Tréhu, A.M., Bohrmann, G., Torres, M.E., and Colwell, F.S. (Eds.)
Proceedings of the Ocean Drilling Program, Scientific Results Volume 204

4. Data Report: Stress Orientation in Gas Hydrate–Bearing Sediments near Hydrate Ridge: Evidence from Borehole Breakouts Observed from Logging-While-Drilling Resistivity Images[1]

D. Goldberg[2] and A. Janik[2,3]

ABSTRACT

We report new observations of borehole breakouts at three sites drilled during Ocean Drilling Program (ODP) Leg 204 in gas hydrate–bearing sediments near Hydrate Ridge on the Cascadia margin. Breakouts are stress-induced features expressed as elongations in the cross-sectional shape of the borehole, caused by compressive failure of the formation under differential horizontal stresses that exceed the formation's in situ strength. Borehole breakouts were detected using an electrical resistivity logging-while-drilling tool (resistivity-at-the-bit tool) in images of the borehole wall, and they occur at two ODP sites located close to the summit of the ridge (Sites 1244 and 1245) and at one site at a greater distance east of the ridge (Site 1251). Based on the orientation of the breakouts, the direction of the in situ maximum horizontal stress (SHmax) was determined at all three sites. We observe SHmax orientations to correspond to localized stresses in the vicinity of Hydrate Ridge (north–northwest–south–southeast at Site 1244 and northeast–southwest at Site 1245), whereas at Site 1251 SHmax appears to roughly correspond to the regional east–west component of the subduction direction.

[1] Goldberg, D., and Janik, A., 2006. Data report: Stress orientation in gas hydrate–bearing sediments near Hydrate Ridge: evidence from borehole breakouts observed from logging-while-drilling resistivity images. *In* Tréhu, A.M., Bohrmann, G., Torres, M.E., and Colwell, F.S. (Eds.), *Proc. ODP, Sci. Results,* 204, 1–14 [Online]. Available from World Wide Web: <http://www-odp.tamu.edu/publications/204_SR/VOLUME/CHAPTERS/108.PDF>. [Cited YYYY-MM-DD]
[2] Lamont-Doherty Earth Observatory of Columbia University PO Box 1000, 61 Route 9W, Palisades NY 10964, USA. Correspondence author: goldberg@ldeo.columbia.edu
[3] Present address: ExxonMobil Exploration Company, PO Box 4778, Houston TX 77210, USA.

Initial receipt: 27 January 2005
Acceptance: 30 January 2006
Web publication: 13 July 2006
Ms 204SR-108

INTRODUCTION

The main objective of this report is to present in situ stress orientation data from borehole breakouts observed in the holes drilled on Hydrate Ridge (Fig. F1) (Tréhu, Bohrmann, Rack, Torres, et al., 2003). Determination of the in situ stress orientation facilitates better understanding of the tectonic regime (i.e., deviatoric stress direction and magnitude) in the vicinity of Hydrate Ridge. Knowledge of the stress regime is also important for evaluating the potential correlation between slope stability and the presence of gas hydrates. Recently, it has been hypothesized that gas hydrate decomposition may be a factor in generating weakness in continental margin sediments, leading to slope failures (e.g., Henriet and Mienert, 1997; Paull et al., 1996, 2000; Janik et al., 2004; Hill et al., 2004). If that is the case, the physical conditions controlling the in situ strength of gas hydrate–bearing formations (i.e., temperature and pressure) have to be fully understood. The in situ pressure is closely related to the in situ stress regime, so its assessment is a prerequisite for further studies linking gas hydrate decomposition to slope stability. Although all observed breakouts occurred below the gas hydrate in these holes, determining the stress directions below the gas hydrate stability zone is particularly relevant to the overall analysis of the stress regime (Goldberg et al., 2003, 2004; Janik et al., 2004).

F1. Regional tectonic setting of Leg 204, p. 8.

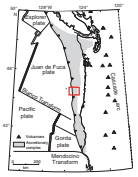

BACKGROUND AND METHODS

During Ocean Drilling Program Leg 204, 10 sites were drilled and logged on Hydrate Ridge of the Oregon continental margin (Tréhu, Bohrmann, Rack, Torres, et al., 2003). Hydrate Ridge is a 25-km-long and 15-km-wide ridge in the Cascadia accretionary complex, formed as the Juan de Fuca plate subducts obliquely beneath North America at a rate of ~4.5 cm/yr. Hydrate Ridge is bound at its northern and southern ends by the left-lateral strike-slip Daisy Bank and Alvin Canyon faults (Goldfinger et al., 1997). The geometry and slip direction of these faults in conjunction with oblique subduction is likely responsible for clockwise rotation of Hydrate Ridge and spatial distribution of deformation zones in the region (Goldfinger at al., 1997; Johnson et al., 2003). The eastern edge of the block occurs at the contact with the Siletz terrain (Fleming and Tréhu, 1999), which forms a backstop for the accretionary prism. Figure F1 shows the general location and tectonic setting of Hydrate Ridge. From Leg 204 coring data, sediments on Hydrate Ridge are known to be composed of clays and silty turbidites and to contain high concentrations of gas hydrates (Tréhu et al., 2004).

Resistivity-at-the-Bit Tool

During Leg 204, geological features were observed in borehole images collected using an electrical resistivity logging-while-drilling (LWD) tool, specifically the resistivity-at-the-bit (RAB) tool (Tréhu, Bohrmann, Rack, Torres, et al., 2003). The RAB tool makes azimuthal resistivity and gamma ray measurements while drilling. Using an azimuthal positioning system, measurements are acquired around the borehole to create a high-resolution, 360° resistivity image of the drilled hole, similar to the wireline Formation MicroScanner (FMS) tool but with complete coverage of the borehole walls (Lovell et al., 1995). Besides the full coverage of the borehole wall, an advantage of the RAB tool is that measure-

ments are collected by an LWD recording device only 3–5 min after drilling and the borehole and formation have less time to deteriorate. Consequently, features observed in the resistivity images better reflect the in situ state of the formation at the time the measurement is taken (Goldberg, 1997).

The RAB tool is connected directly above the drill bit. The lower portion of the tool and the bit itself take a variety of resistivity measurements (Fig. F2). Button electrodes provide shallow-, medium-, and deep-focused resistivity measurements acquired with ~6° (1.4 cm) azimuthal resolution. The RAB tool rotates during drilling to produce azimuthally oriented images with 360° coverage of the borehole wall. The button electrodes are ~1 in (2.5 cm) in diameter, and they provide depths of investigation of ~1, 3, and 5 in (2.5, 7.6, and 12.7 cm), respectively. The vertical sampling resolution of the image is typically 3–4 cm. The tool's orientation system uses Earth's magnetic field as a reference to determine its position with respect to the borehole. RAB resistivity images can reveal information about formation structure, lithologic contacts, natural fractures, and borehole breakouts. In this paper, we analyze RAB resistivity images to quantify the orientation of borehole breakouts observed at the Leg 204 sites.

F2. LWD tool string and RAB tool, p. 9.

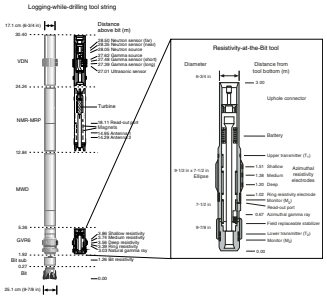

Borehole Breakouts and Estimation of Stress Orientation

Borehole breakouts are stress-induced features expressed as elongations in the cross-sectional shape of the borehole (Bell and Gough, 1979, 1983). When a borehole is drilled, the material removed from the subsurface no longer supports the surrounding rock. As a result, the hoop stresses become concentrated around the borehole wall (Kirsch, 1898; Jaeger and Cook, 1979). If the concentration of the hoop stress exceeds the formation's in situ compressive strength, tangential shear failures ensue and generate spalling along the interior of the borehole (Fig. F3A) on opposite sides of a borehole, centered at the azimuth of the horizontal minimum principal stress, and at the locus of the maximum concentration of hoop stress around the borehole (Zoback et al., 1985; Moos and Zoback, 1990; Barton et al., 1997; Ask, 1997; Brudy and Kjorholt, 2001). Spalling occurs at diametrically opposed points on the borehole wall, aligned with the direction of the minimum principal stress, SHmin, and perpendicular to the maximum principal stress, SHmax. Knowing this antipodal relationship, we can use the breakout orientation as a reliable indicator of the local maximum principal horizontal compressive stress direction in the vertical boreholes.

The RAB resistivity tool can be utilized to detect breakouts even though it does not directly measure the borehole diameter/elongation (McNeill et al., 2004). The enlarged cross-section of the borehole due to spalling introduces more fluid between the RAB sensors and the formation, which appear as zones of lower resistivity and higher apparent porosity in the RAB resistivity image (Fig. F3B). In addition, sediments in the vicinity of the breakouts may have higher porosity, and thus lower resistivity, due to small-scale fracturing and seawater invasion in the formation.

F3. Borehole cross section and breakouts, p. 10.

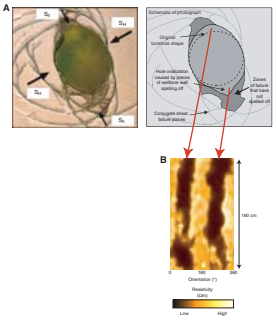

RESULTS

During Leg 204, breakouts were observed in RAB images at two sites located close to the summit of Hydrate Ridge (Sites 1244 and 1245) and at one site east of the ridge (Site 1251). The breakouts are generally fairly continuous with some intermittent intervals related perhaps to lithologic controls. Sites 1244 and 1245 have breakout occurrences starting at depths of 249 and 217 meters below seafloor (mbsf), respectively, extending to the total hole depths. At Site 1251, breakouts occur at 161 mbsf to its total depth. Figure **F4** illustrates the depth extent of breakouts and gas hydrate stability at these three sites. Azimuths of the measured breakouts are statistically averaged over the entire depth interval where they occur. These analyses were computed with GMImager software using Mardia statistics for the directional data (Mardia, 1972). GMImager results are shown in Figure **F5.** Average azimuths of the breakouts are presented in Table **T1.**

The measured azimuths at each site are considered statistically constant, yielding the orientation of the minimum horizontal stress direction (SHmin) in each hole. SHmax can then be determined by computing the azimuth at perpendicular orientations. These azimuths are also shown in Table **T1.** Given the shallow penetration depths of these sites, we infer that SHmax direction measured below the gas hydrates most probably can be extrapolated up to the shallower part of the borehole to the gas hydrate stability zone.

Figure **F6** illustrates SHmax in the context of the regional tectonics (Johnson et al., 2003). At Site 1245, SHmax is observed to be oriented northeast–southwest (ridge subparallel, with an east trend), and at Site 1244, SHmax is north–northwest–south–southeast (also ridge subparallel, with a west trend). The ridge-subparallel direction of SHmax can be related to the tectonic alignment and localized stresses near Hydrate Ridge, which involve a central uplift of the ridge and consequent normal faulting on its flanks (Figs. **F4A, F6A**). Those stress directions also correspond with the orientation of fractures identified in the RAB images and core recovered during Leg 204 (J.L. Weinberger, pers. comm., 2004). It has to be noted, though, that breakouts at Sites 1245 and 1244 occur in two different lithologic units (Fig. **F4A**), so lithologic controls cannot be entirely excluded. At Site 1251, located east and more distant from the ridge summit, SHmax is oriented east–southeast–west–northwest. This orientation appears to be roughly perpendicular (within error) to the edge of the north–south oriented Siletz terrain to the east (Fleming and Tréhu, 1999), supporting the suggestion of strain partitioning into margin-normal compression and margin-parallel strike-slip component, west of the backstop (McNeill et al., 2000). The localized ridge-aligned stress associated with the central uplift and normal faulting near the summit is less significant at this location.

ACKNOWLEDGMENTS

We thank GeoMechanics International, Inc., for access to their GMImager software and Judith Sheridan for her technical efforts. We also thank Dan Moos and Johanna Chevalier for their insightful discussions. Joel Johnson provided the structural map in Figures F1 and F6B, and Jill Weinberger provided her LWD-based fracture analyses at Leg 204 sites. This research used data provided by the Ocean Drilling Program (ODP). ODP is sponsored by the U.S. National Science Foundation

F4. Seismic reflection profiles, p. 11.

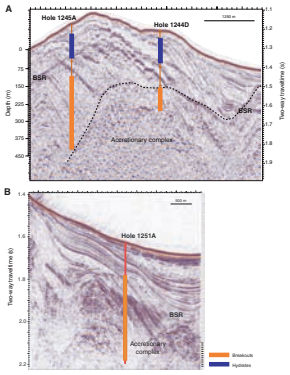

F5. Azimuth of borehole breakouts, p. 12.

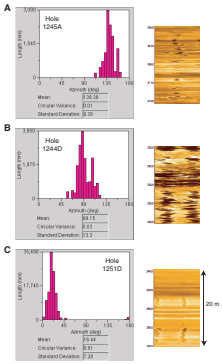

T1. Azimuth of breakout orientations, p. 14.

F6. Maximum horizontal stress direction and structural map, p. 13.

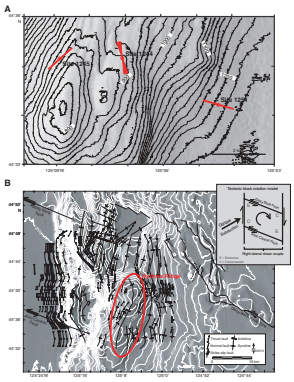

(NSF) and participating countries under management of Joint Oceanographic Institutions (JOI) Inc. Funding for this research was provided by the U.S. Department of Energy (DOE) and JOI/NSF. Lamont-Doherty Publication Number 6927.

REFERENCES

Ask, M.V.S., 1997. In situ stress from breakouts in the Danish sector of the North Sea. *Mar. Pet. Geol.,* 14:231–243. **doi:10.1016/S0264-8172(97)00007-X**

Barton, C.A., Moos, D., Peska, P., and Zoback, M.D., 1997. Utilizing wellbore image data to determine the complete stress tensor: application to permeability anisotropy and wellbore stability. *Log Anal.,* 38:21–33.

Bell, J.S., and Gough, D.I., 1979. Northeast-southwest compressive stress in Alberta: evidence from oil wells. *Earth Planet. Sci. Lett.,* 45:475–482.

Bell, J.S., and Gough, D.I., 1983. The use of borehole breakouts in the study of crustal stress. *In* Zoback, M.D., and Haimson, B.C. (Eds.), *Hydraulic Fracturing Stress Measurements:* Washington (National Academy Press), 201–209.

Brudy, M., and Kjørholt, H., 2001. Stress orientation on the Norwegian continental shelf derived from borehole failures observed in high-resolution borehole imaging logs. *Tectonophysics,* 337:65–84. **doi:10.1016/S0040-1951(00)00299-7**

Clague, D., Maher, N., and Paull, C.K., 2001. High-resolution multibeam survey of Hydrate Ridge, offshore Oregon. *In* Paull, C.K., and Dillon, W.P. (Eds.), *Natural Gas Hydrates: Occurrence, Distribution, and Detection.* Geophys. Monogr., 124:297–306.

Fleming, S.W., and Tréhu, A.M., 1999. Crustal structure beneath the central Oregon convergent margin from potential field modeling: evidence for a buried basement ridge in local contact with a seaward dipping backstop. *J. Geophys. Res.,* 104(B9):20431–20447. **doi:10.1029/1999JB900159**

Goldberg, D., 1997. The role of downhole measurements in marine geology and geophysics. *Rev. Geophys.,* 35:315–342. **doi:10.1029/97RG00221**

Goldberg, D., Guerin, G., Janik, A., and Collett, T., 2004. Heterogeneity and strength of natural gas hydate–bearing sediments. *Search Discovery,* 90035. Available from World Wide Web: <**http://www.searchanddiscovery.com/documents/abstracts/2004hedberg_vancouver/extended/goldberg/goldberg.htm**>.

Goldberg, D., Janik, A., Johnson, J., Moos, D., Flemings, P., Barr, S., and ODP Leg 204 Shipboard Scientific Party, 2003. Stress orientations and estimated in situ strength of gas hydrate—evidence from borehole breakouts at ODP Leg 204 sites, Hydrate Ridge. *Geophys. Res. Abstr.,* 5:02358.

Goldfinger, C., Kulm, L.D., Yeats, R.S., McNeill, L., and Hummon, C., 1997. Oblique strike-slip faulting of the central Cascadia submarine forearc. *J. Geophys. Res.,* 102(B4):8217–8243. **doi:10.1029/96JB02655**

Henriet, J-P., and Mienert, J. (Eds), 1997. Gas hydrates: relevance to world margin stability and climate change. *Spec. Publ.—Geol. Soc. London,* 137:215–222.

Hill, J., Driscoll, N., Weissel, and Goff, J., 2004. Large scale elongated gas blowouts along the U.S. Atlantic maring. *J. Geophys. Res.,* 109. **doi:10.1029/2004JB002969**

Jaeger, J.C., and Cook, N.G.W., 1979. *Fundamentals of Rock Mechanics* (3rd ed.): New York (Chapman and Hall).

Janik, A., Goldberg, D., Moos, D., Sheridan, J., Flemings, P., Germaine, J., and Tan, B., 2004. Constraints on the strength of the gas hydrate-rich sediments from borehole breakouts—implications for slope stability near Hydrate Ridge on the U.S. continental margin off-shore Oregon. *AAPG Bull Suppl.,* 88:13.

Johnson, J.E., Goldfinger, C., and Suess, E., 2003. Geophysical constraints on the surface distribution of authigenic carbonates across the Hydrate Ridge region, Cascadia margin. *Mar. Geol.,* 202(1–2):79–120. **doi:10.1016/S0025-3227(03)00268-8**

Kirsch, G., 1898. Die theorie der elastizitaet und die bedeurfnisse der festigkeitslehre. *VDI Zeitschrift,* 42:797–807.

Lovell, J.R., Young, R.A., Rosthal, R.A., Buffington, L., and Arceneaux, C.L., Jr., 1995. Structural interpretation of resistivity-at-the-bit images. *Trans. SPWLA Annu. Logging Symp.,* TT.

Mardia, K.V., 1972. *Statistics of Directional Data:* London (Academic Press).

McNeill, L.C., Goldfinger, C., Kulm, L., and Yeats, R., 2000. Tectonics of the Neogene Cascadia forearc basin: investigations of a deformed late Miocene unconformity. *Geol. Soc. Am. Bull.,* 112(8):1209–224.

McNeill, L.C., Ienaga, M., Tobin, H., Saito, S., Goldberg, D., Moore, J.C., and Mikada, H., 2004. Deformation and in situ stress in the Nankai accretionary prism from resistivity-at-bit images, ODP Leg 196. *Geophys. Res. Lett.,* 31. **doi:10.1029/2003GL018799**

Moos, D., and Zoback, M.D., 1990. Utilization of observations of well bore failure to constrain the orientation and magnitude of crustal stresses: application to continental, Deep Sea Drilling Project, and Ocean Drilling Program boreholes. *J. Geophys. Res.,* 95:9305–9325.

Paull, C.K., Buelow, W.J., Ussler, W., III, and Borowski, W.S., 1996. Increased continental-margin slumping frequency during sea-level lowstands above gas hydrate-bearing sediments. *Geology,* 24:143–146. **doi:10.1130/0091-7613(1996)024<0143:ICMSFD>2.3.CO;2**

Paull, C., Ussler, W., and Dillon, W., 2000. Potential role of gas hydrate in generating submarine slope failures. *In* Max, M. (Ed.), *Natural Gas Hydrate in Oceanic and Permafrost Environments:* Amsterdam (Klewer), 149–156.

Reinecker, J., Tingay, M., and Mueller, B., 2003. Borehole breakout analysis from the four-arm caliper logs. In *World Stress Map Project—Guidelines: Four-arm Caliper Logs* [Online]. Available from World Wide Web: <**http://www-wsm.physik.uni-karlsruhe.de/pub/guidelines/BOanalysis_4armcaliper.pdf**>.

Tréhu, A.M, Bohrmann, G., Rack, F.R., Torres, M.E., et al., 2003. *Proc. ODP, Init. Repts.,* 204 [Online]. Available from World Wide Web: <**http://www-odp.tamu.edu/publications/204_IR/204ir.htm**>.

Tréhu, A.M., Long, P.E., Torres, M.E., Bohrmann, G., Rack, F.R., Collett, T.S., Goldberg, D.S., Milkov, A.V., Riedel, M., Schultheiss, P., Bangs, N.L., Barr, S.R., Borowski, W.S., Claypool, G.E., Delwiche, M.E., Dickens, G.R., Gracia, E., Guerin, G., Holland, M., Johnson, J.E., Lee, Y.-J., Liu, C.-S., Su, X., Teichert, B., Tomaru, H., Vanneste, M., Watanabe, M., and Weinberger, J.L., 2004. Three-dimensional distribution of gas hydrate beneath southern Hydrate Ridge: constraints from ODP Leg 204. *Earth Planet. Sci. Lett.,* 222:845–862. **doi:10.1016/j.epsl.2004.03.035**

Zoback, M.D., Moos, D., Mastin, L., and Anderson, R.N., 1985. Well bore breakouts and in situ stress. *J. Geophys. Res.,* 90:5523–5530.

Figure F1. Regional tectonic setting of Leg 204 in the accretionary prism of the Cascadia subduction zone (Tréhu, Bohrmann, Rack, Torres, et al., 2003).

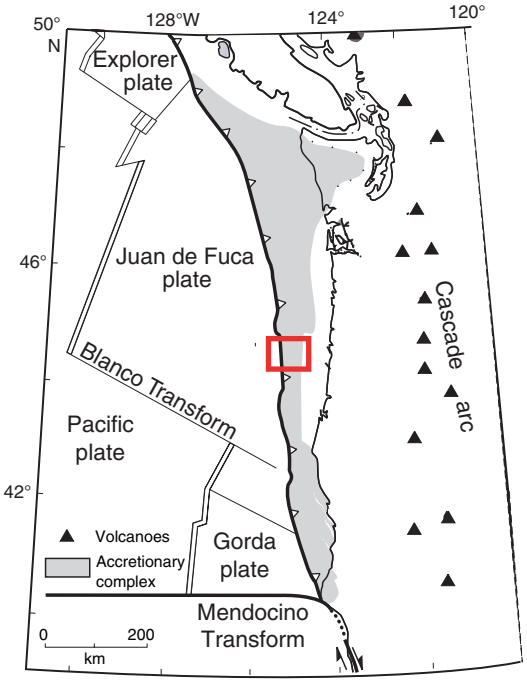

Figure F2. Schematic of the logging-while-drilling (LWD) tool string with details of the resistivity-at-the-bit (RAB) tool. VDN = Vision Neutron Density tool, NMR-MRP = Nuclear Magnetic Resonance tool, MWD = measurement-while-drilling tool, GVR = GeoVision Resistivity tool.

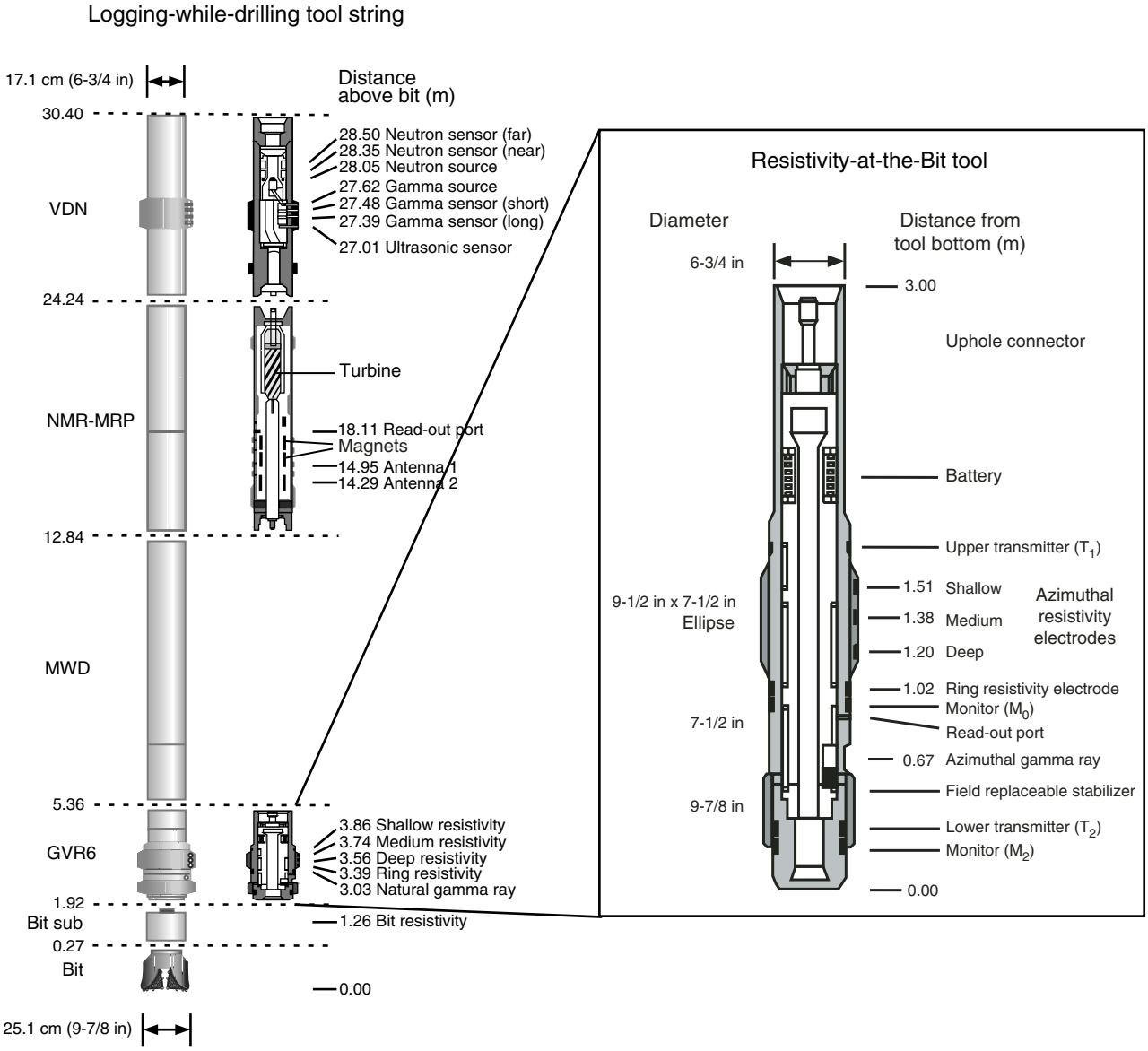

Figure F3. A. Plan view of borehole cross section from laboratory tests performed on the hollow cylinder of rock, showing borehole breakout caused by intersection of conjugate shear failure planes that result in an enlargement of the cross-sectional shape of the cylinder (Reinecker et al., 2003). SHmax (S_H) and Shmin (S_h) refer to the orientations of maximum and minimum horizontal stress, respectively. **B.** RAB resistivity image showing borehole breakouts manifested as dark vertical bands of lower electrical resistivity.

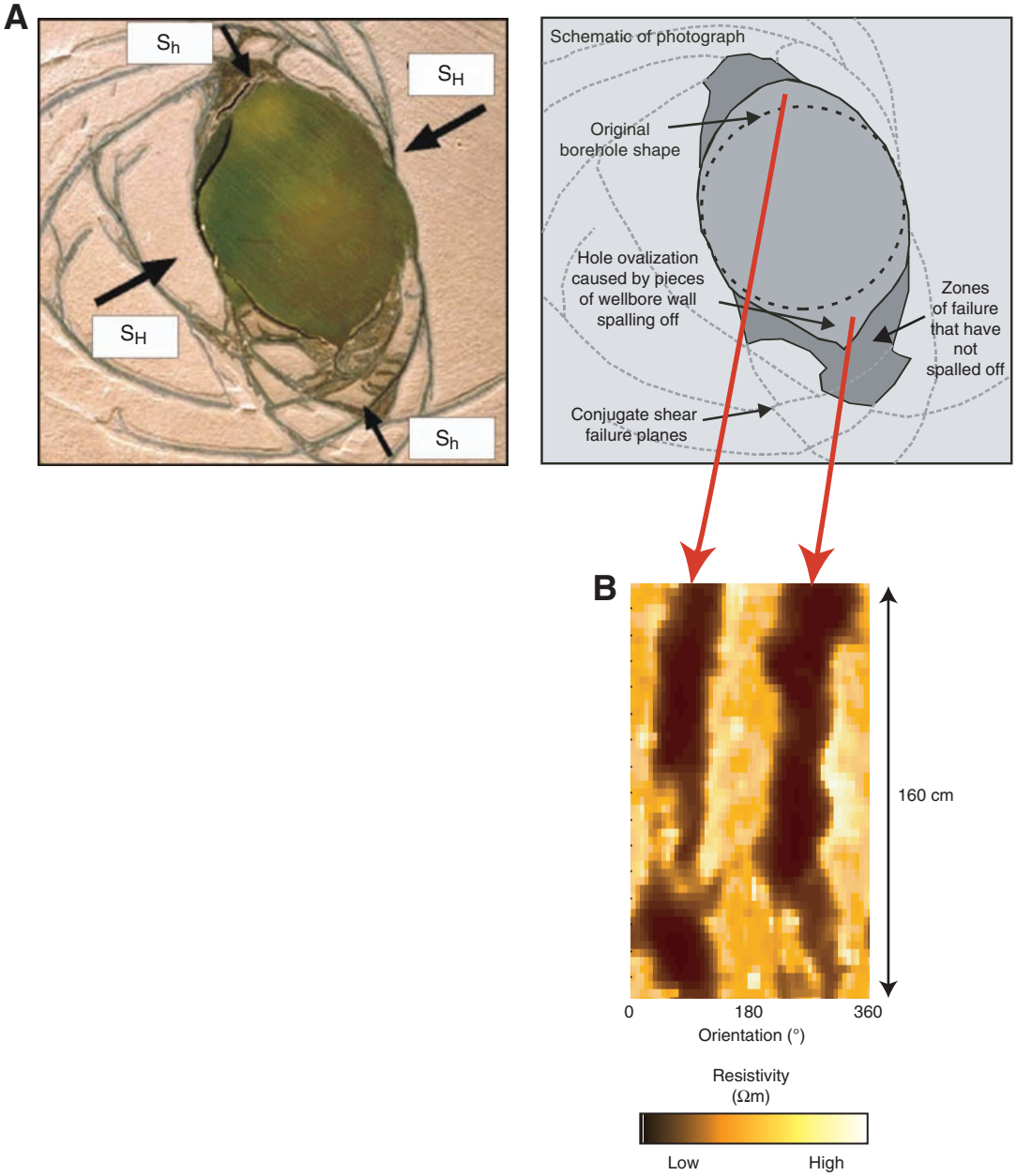

Figure F4. Seismic reflection profiles crossing near (**A**) Holes 1245A and 1244D, and (**B**) Hole 1251A. Approximate intervals of breakouts and gas hydrates occurrences (gas hydrate stability zone) are indicated. Dashed line indicates the boundary between the accretionary complex and overlying sediments. Uncertainties in depth-time conversion of these seismic sections are approximately ±5–10 m. BSR = bottom-simulating reflector.

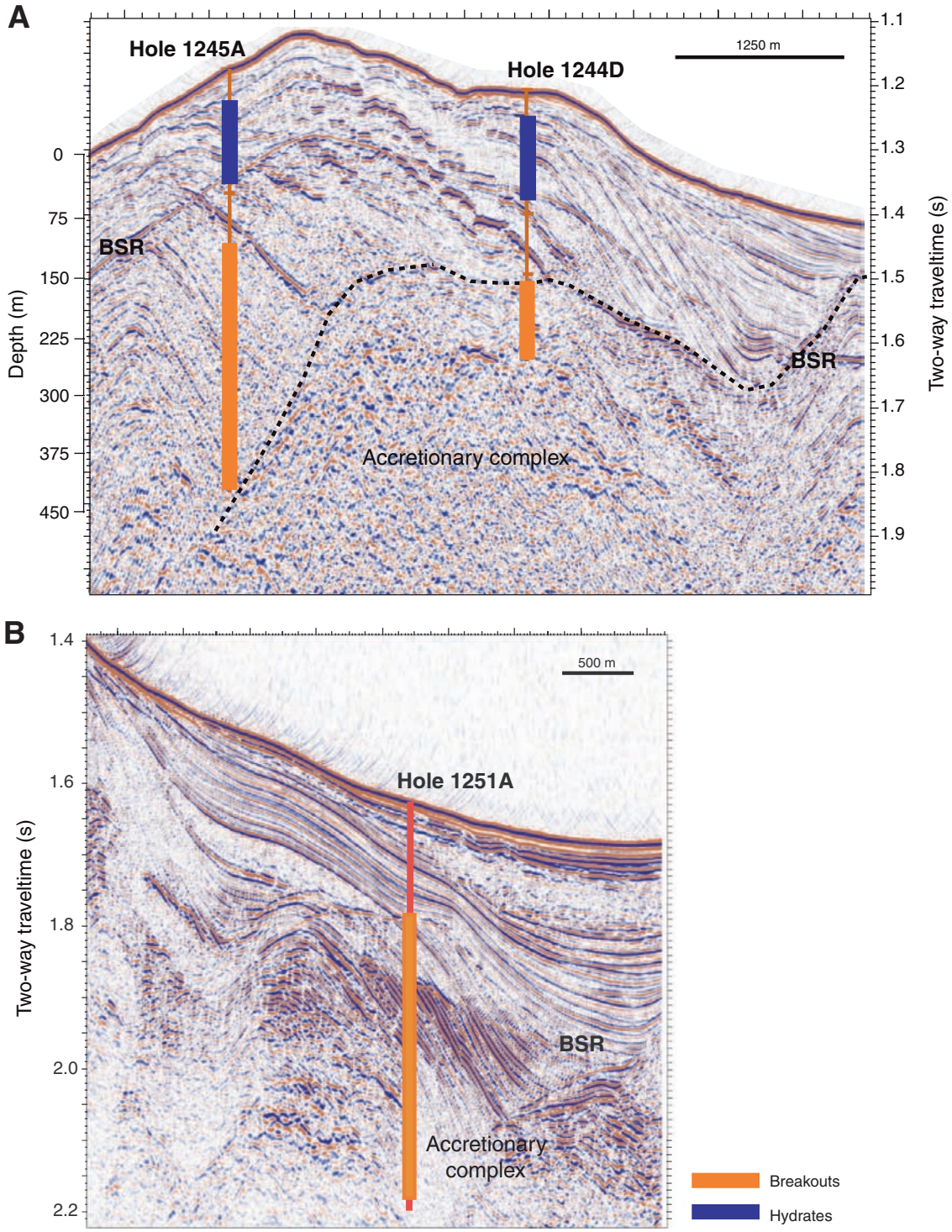

Figure F5. Histograms computed using GMImager software of the azimuth of borehole breakouts occurring in (**A**) Hole 1245A, (**B**) Hole 1244D, and (**C**) Hole 1251A. RAB images over 20-m intervals illustrate typical borehole breakouts observed in each of these sedimentary sections.

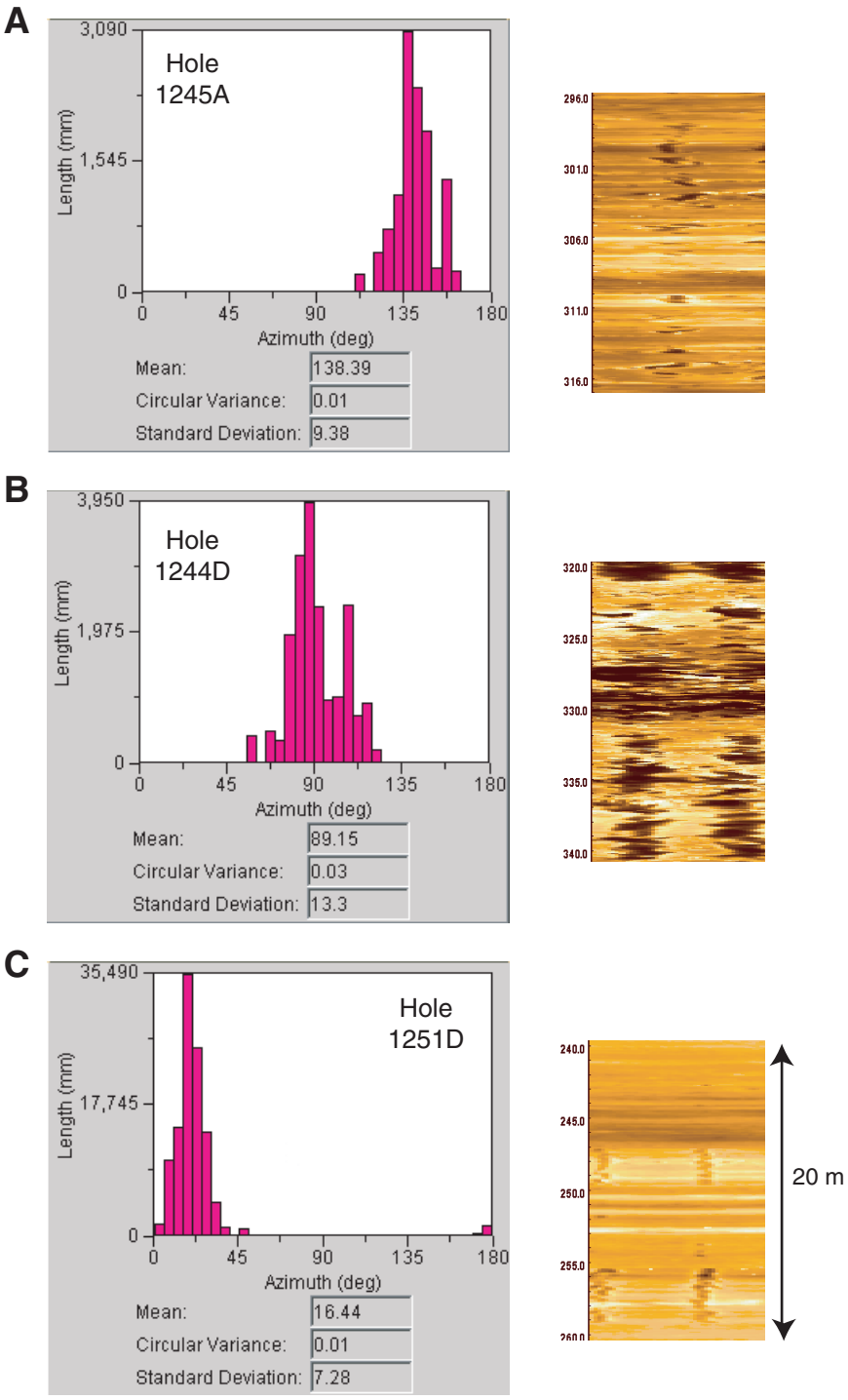

Figure F6. A. Maximum horizontal stress direction in Holes 1245A, 1244D, and 1251A plotted on a bathymetry map of near Hydrate Ridge (after Clague et al., 2001). **B.** Detailed structural map of the Hydrate Ridge region interpreted from multichannel seismic reflection profiles and overlain on 100-m shaded relief bathymetry (Goldfinger et al., 1997; Johnson et al., 2003). Deep-seated left-lateral strike-slip faults (Daisy Bank and Alvin Canyon faults) dominate the deformation north and south of Hydrate Ridge, and thrusts and folds are common in the region between the strike-slip faults. Inset shows a structural interpretation of the Hydrate Ridge region, with apparent clockwise rotation relative to the deformation front, and suggests that deformation is dominated by oblique subduction-driven shear. SHR = southern Hydrate Ridge.

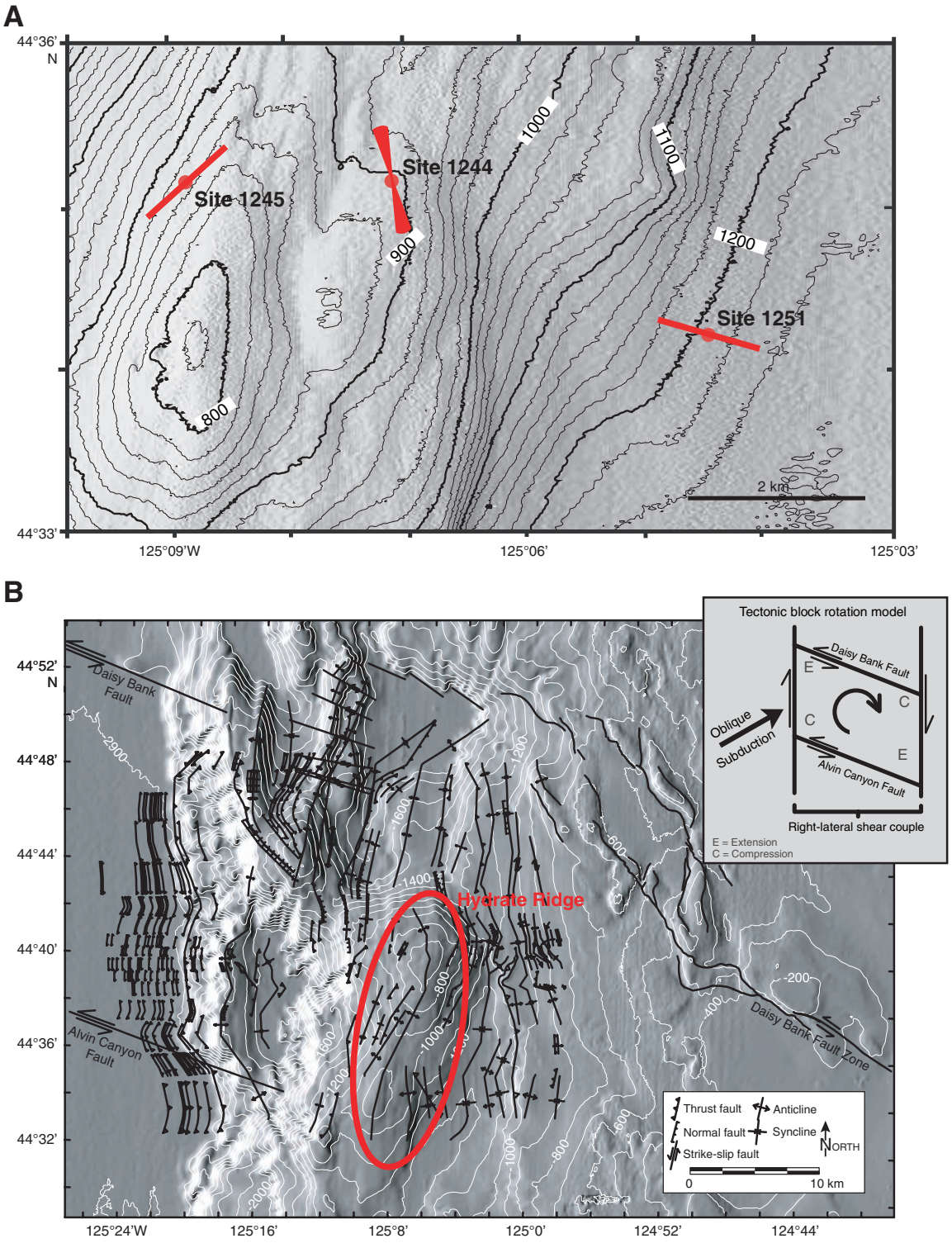

Table T1. Azimuth of breakout orientations.

Site	Breakout azimuth (°)	Standard deviation (°)	SHmax azimuth (°)
1244	89	13	179
1245	138	9	48
1251	16	6	106